Artificial Neural Network for the provenance study of archaeological ceramics using clay sediment database

Germana Barone[1], Paolo Mazzoleni[1], Grazia Vera Spagnolo[2], Simona Raneri[3]

[1] *University of Catania, Department of Biological, Geological and Environmental Sciences, C.so Italia 57 - 95129 Catania (Italy)*

[2] *University of Messina, Department of ancient and modern civilization, Polo Universitario SS Annunziata98168, Messina (Italy)*

[3]*University of Pisa, Department of Earth Science, Via Santa Maria 53 - 53126 Pisa (Italy)*

**corresponding author: pmazzol@unict.it*

Abstract

An artificial neural network (**A**NN) for archaeometric studies was created to facilitate provenance attribution of archaeological ceramics. A multilayer perceptron model (MLP) was applied to construct the network, including only one hidden layer. Moreover, correction parameters based on historical and archaeological evidences were applied to Bayesian probability factor.

The **A**NN **was** trained by using clays mixings mathematically constructed **based on** a reference chemical database of Sicilian sediments. The clay mixing takes in consideration compositional variability within the same geological site and **the extent of the** ceramic **manufacture** processes. Test was performed by querying the **A**NN with compositional data of ceramics found in archaeological sites coherent with clays sampling areas. Up to 88% correct attribution was verified, with **good** correspondence between geological and archaeological contexts.

Finally, merits of **A**NN were highlighted **by** comparing the extent of successfully provisional attribution with classical statistical method**s** (PCA and LDA).

Keywords: ANNs; archaeometry; pottery; clayey sediments; geochemistry; production sites; provenance.

Graphical abstract

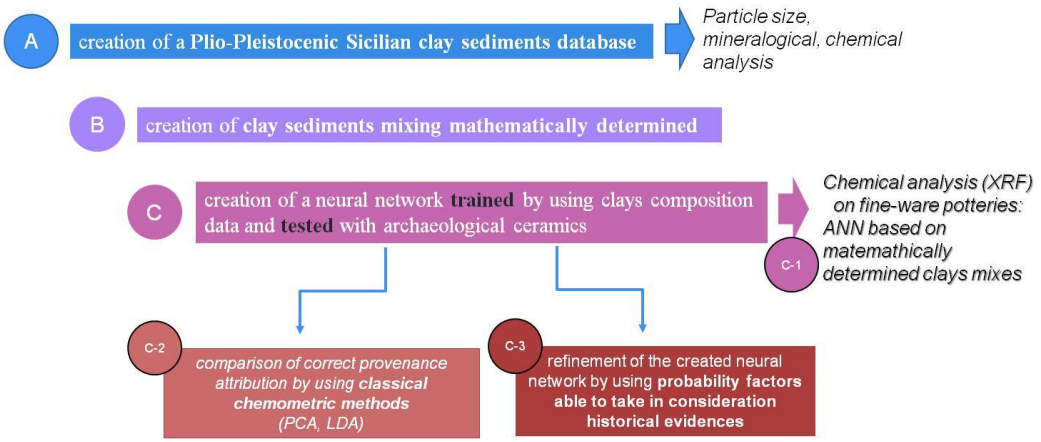

1. Introduction

The identification of the production sites in archaeological ceramics studies represent a key factor in reconstructing both economic and cultural history of ancient communities; in view of their daily use, pottery allows in fact to derive significant information on land resources, trade, customs, behaviors and religious beliefs. Provenance studies of archeological ceramics usually deal with compositional data; **comparative studies** between ceramics and reference clayey raw materials or laboratory experimental mixes are often **carried out** to locate production centers **and draw possible** imports routes [1–5]. However, these predictions are not always trivial, because of the extent of production process **[6]. Thus, comparative evaluations between possible raw materials and artefacts have to take in account the possible mixing of clay sediments sampled in one or more outcrops, the intentional addition of tempers or the depuration of the sediment for technical purposes.** T**ying to model the final composition of a certain ceramic artifact by considering all factors proper of the production cycle, it can be expressed by** the following equations:

For **a simple ware (no addition, no depuration)**: $C_i^p = \sum_{j=1}^{n} X^{s(j)} C_i^{s(j)} + H_2O$ (1)

For **potteries with added tempers**:$C_i^p = \sum_{j=1}^{n} X^{s(j)} C_i^{s(j)} + X^t C_i^t + H_2O$ (2)

For **depurated potteries**: $C_i^p = \sum_{j=1}^{n} X^{s(j)} C_i^{s(j)} - X^c C_i^c + H_2O$ (3)

where C_i^p is the abundance of **aplastic fraction** *i* in the ceramic paste; $X^{s(j)}$ the mass fraction of clayey sediment *s(j);* $C_i^{s(j)}$ the abundance of **aplastic fraction** *i* of the clayey sediment *s(j)*; X^t the mass fraction of temper; C_i^t the abundance of **aplastic fraction** *i* of temper; X^c the mass fraction of coarse grain size of clayey sediments; C_i^c the abundance of **aplastic fraction** *i* of coarse grain size; H_2O mixing water.

In the field of arch**a**eological sciences, compositional data are often obtained by X-ray fluorescence analysis (XRF). The management and processing of large chemical dataset available from such instrumental analysis is usually addressed by the application of **statistical** methods for predicting groups and/or relations among samples [7]. Literature offers a large overview on different statistical procedures useful to address provenance issues in XRF data analysis related to archaeological ceramics, including principal component analysis (PCA), factor analysis (FA), linear discriminant analysis (LDA), cluster analysis (HCA) [8–19], even discussing possible limits and drawbacks [7].

Among the most popular **statistical** methods, artificial neural networks (ANNs) has been recently proposed as particularly challenging in archaeological applications to optimize predictions and correlations among objects [20–23]. However, the complex computational process and the relevant amount of samples required in training neutral networks generally favor the use of other classical methods. Artificial Neural Networks (ANNs) were developed for the first time by McCulloch & Pitts [24]. The definition of an ANN frequently recurs to parallelism with biological paradigms, resembling its structure the brain's architecture and the human learning

procedures. According to [25], "*A neural network is a massively parallel distributed processor made up of simple processing units, which has a natural propensity for storing experiential knowledge and making it available for use. It resembles the brain in two respects: 1) knowledge is acquired by the network from its environment through a learning process; 2) inter neuron connection strengths, known as synaptic weights, are used to store the acquired knowledge*".

An ANN is due to simple processing units named neurons, acting as nerve cells able to receive inputs, elaborate them by specific operations and exchange output results with the other connected processing elements.

The structure of a simple ANN consists in layers of neurons, the first of which is the input layer while the last one is an output layer **(see Figure 1.a); i**n the middle, one or more hidden neuron layers **may be present** (Figure 1.b).

In a feedforward ANN, the information flux occurs always from the input layer to the output one.

An artificial neuron works by calculating a weighted sum of external inputs ($x_{k1.....n}$) and adding constants (bias – b_k) to generate an intermediate v_k function for which connections have to be still verified.

$$v_k = \sum_{j=0}^{n} w_{kj} x_j \qquad (4)$$

This step is governed by the application of an activation function (e.g. φ(*v*)) able to activate (or not) a connection and finally give back an output answering to a specific query. Usually, a sigmoid activation function is used in ANN construction (Figure 1.c); its values range from 0 to +1 and it is mathematically defined by the equation:

$$\varphi(v) = 1/(1 + e^{-av}) \qquad (5)$$

where *a* is the slope parameter of the sigmoid function. Another activation function widely used is the hyperbolic tangent function ($\varphi(v) = \tanh(v)$) , which values range from -1 to +1.

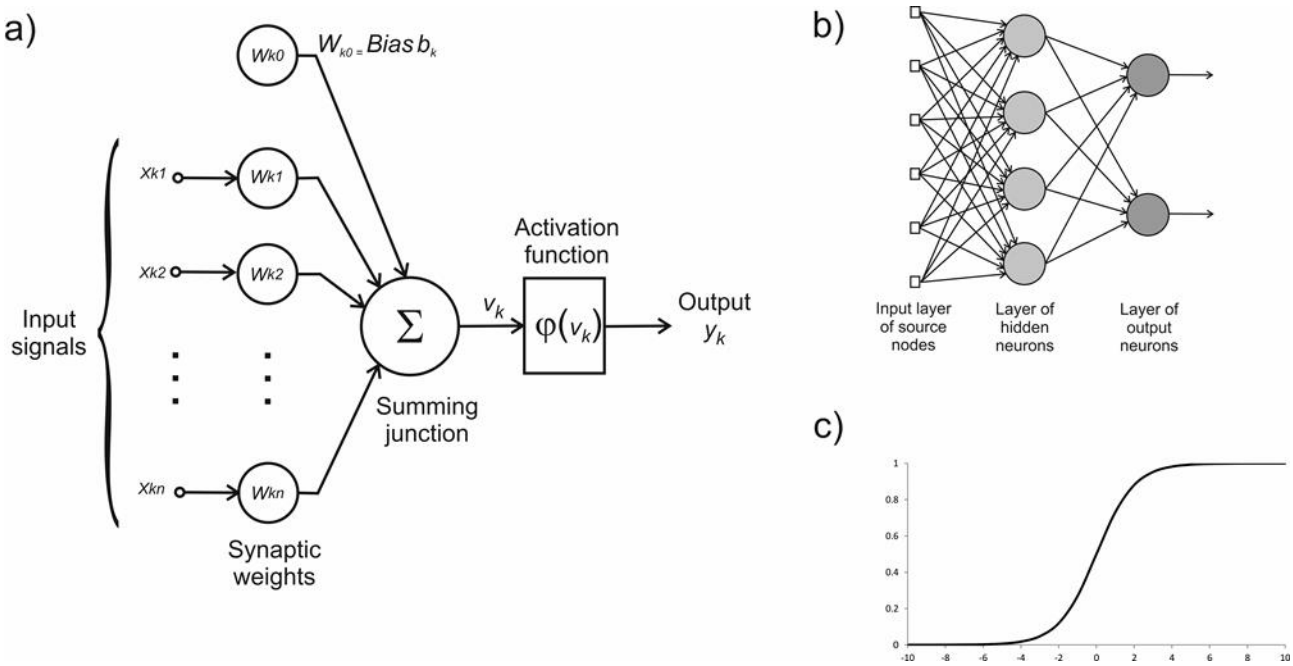

Figure 1. (a) Schematic representation of **A**NN architecture and basic operations, **(b) example of a simple feed forward ANN consisting in three neuron layers and** (**c**) example of sigmoidal activation function and (modified from [26]).

The main feature of neural network is its ability to learn from its environment and to improve its performance through **consecutive** learning **steps (i.e., adjustments applied to weight sums and bias and/or application of correction factors)**. **Two different** learning process **can be used**: i) supervised learning, in which the network is trained by providing **known information as** inputs and **by** matching output patterns; ii) unsupervised learning, in which output units are trained **creating correlation with groups into the input series,** without a priori set of categories into which the patterns are classified. The learning process is achieved undergoing a training session. **A** set of input patterns along with the category to which each particular pattern belongs is repeatedly **submitted** to the network**; thus,** the prediction ability of the network **can be** verified by **testing** an unclassified pattern, which classification criteria are extracted from the training data.

ANNs **activate a certain number of correlations** by subdividing the multidimensional decision space into regions, each one associated with a class. The decision boundaries are determined **within** the training process and the construction of these boundaries is **based on** the inherent variability within and between classes. Specifically, an **A**NN without hidden layer produces a linear decision boundary (Figure 2.a) (likewise in linear discriminant analysis); on the contrary, one or more hidden layer (named multi layers neural network – MLNN) permit to obtain a non-linear decision boundary (Figure 2.b).

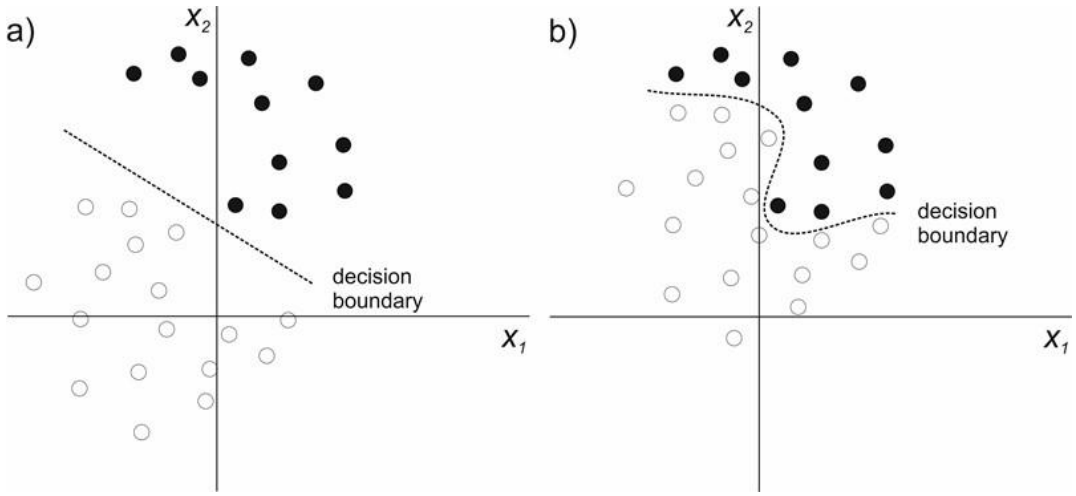

Figure 2. Decision boundaries determined in case of (a) absence or (b) presence of hidden layers.

The basis of the ANN computational model clarify its advocacy to every possible scientific field, including archeological datasets. Nevertheless, comprehensive studies able to point out merits of neural network in comparison of other multivariate analysis are largely lacking [7,27].

To fill this gap and demonstrate potential of **A**NNs in archeological researches, especially for provenance attribution of archaeological ceramics, an artificial neural network based on clay sediments compositional database was trained **and successfully tested. In detail, the learning process was carried out** considering mathematically determined clay mixings of Plio-Pleistocene Sicilian clays, extensively employed in ancient times to produce ceramics [11,28–33]. Thus, the prediction ability of the **A**NN in classifying ceramics was tested on selected artifacts previously **studied and classified** [11,28–30,34,35]**. Finally, merits of the method were explored by comparing ANN results with** other classical statistical methods (PCA and LDA).

2. Research aim

The creation of a (i) Plio-Pleistocenic Sicilian clay sediments database, (ii) clay sediment mixings mathematically determined and (iii) a**n artificial** neural network trained by using clays composition data and tested with archaeological ceramics represents the workflow steps of this research, finalized to improve provisional attribution based on chemical composition. The main aim of this study is therefore to test the neural network approach using reference groups of ceramics materials already characterized by archaeometric studies and identified as certain local productions, avoiding a priori assumptions. The comparison of correct provenance attribution obtained by using different **statistical methods**, and the final refinement of the created neural network by using probability factors able to take in consideration historical and archaeological evidences, highlighted merits of ANNs in archaeometric studies **of** archeological ceramics.

3. Materials

3.1 Clay sediments

Plio-Plestocenic clays and marly clay sediments were considered to create mathematically determined clay mix**es** and **to** train **the artificial** neural network. From the geological point of view, these clays represent a sedimentation phase occurred in submerged areas during Pliocene and Pleistocene, after the main Miocenic phase of orogenic building of the Sicilian chain, and the Messinian Salinity crisis [36]. Plio-Pleistocenic clays **(Figure 3)** were deposited in different tectonic setting (forearc, piggy back and foreland basins) [37] and geographic context of Sicily, being therefore widely available through the island.

For this study, **65 samples of** Plio-Plestocenic clays belonging to different geological **Fm.** and outcropping in different areas of the east and south Sicily were sampled and analysed:

i) Rometta Fm. (Upper Pliocene – Lower Pleistocene) sampled near Tracoccia and Barcellona 10 km from Milazzo; 14 samples;

ii) Bluish Clay Fm. (Lower – Middle Pleistocene) sampled near Catania, Aci Trezza (10 km from Catania) and Sferro (25 km from Catania); 10 samples

iii) Bluish Clay Fm. (Lower – Middle Pleistocene) sampled near Lentini; 13 samples;

iv) Bluish Clay Fm. (Lower – Middle Pleistocene) sampled near Siracusa; 10 samples;

v) Mt. Narbone Fm (Middle – Upper Pliocene) sampled near Gela; 8 samples;

vi) Mt. Narbone Fm (Middle – Upper Pliocene) sampled near Agrigento; 10 samples.

The studied clays outcrop on different geological environments [37]: (i) on high-medium grade metamorphic basement, in Milazzo area; ii) on volcanic edifice, in Catania (on the slopes of Mt. Etna); iii) on basaltic lava cover and limestone sequences, in foreland setting in Lentini territory; iv) in foreland area characterized by limestone sequences, in Siracusa; and v) at the front of the Sicilian trust belt, in Gela and Agrigento.

These geological Fm. were extensively used for local ceramic manufacture in antiquity; however, compositional overlapping among different Fm. as well as compositional difference within the same site due to genetic reasons can determine relevant uncertainties in provenance studies.

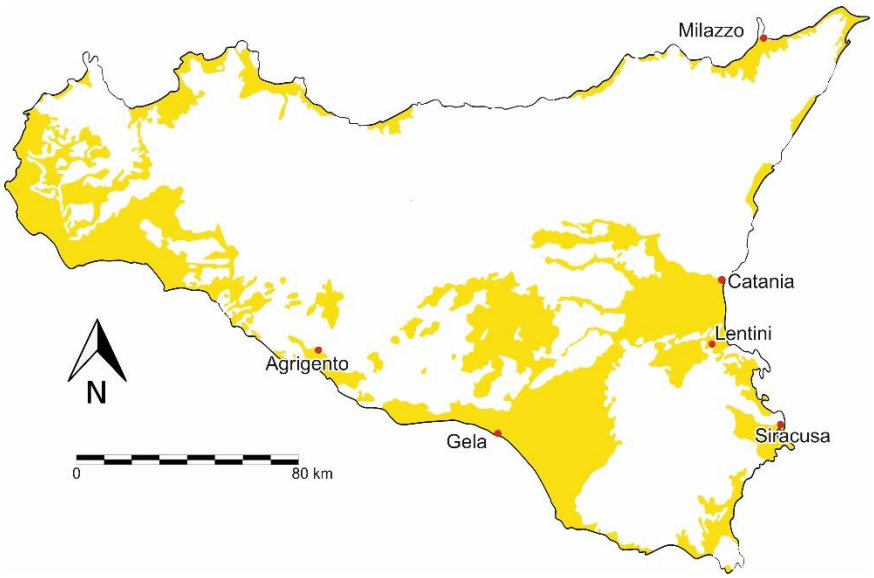

Figure 3. Geological sketch map showing the distribution of Sicilian Plio-Pleistocene clays and marly clay sediments. For a complete description of the geological Formations constituting these sedimentary basins see [37]. The sampling areas are reported in the map.

3.2 Ceramics

The neural network was tested by **an** unclassified pattern consisting in 118 pottery samples with medium and fine grain size to avoid miscalculations in the computational process due to the occurrence of tempers intentionally added in the clay paste. They include ancient ceramics characterized in previous studies by using classical minero-petrographic and chemical methods allowing certain attribution as local reference groups of different Greek colonies of Sicily (Milazzo, Catania, Lentini, Siracusa, Gela, Agrigento). **Previous studies have in fact demonstrated the use of local Plio-Pleistocenic sediments in manufacturing these artefacts. For this reason, the different ceramic groups from the Greek colonies reflect, in their chemical composition, the variability of the employed geological sources and the already discussed compositional overlap.**

In detail, they account the following productions: i) black glazed pottery, dated from VI to III B.C., from Milazzo **(11 samples)** [35]; black glazed pottery **(10 samples) and common ware (11 samples)** of the hellenistic period from Catania [11]; common ware of the hellenistic period from Lentini [11] **(32 samples)**; black glazed pottery **(6 samples)**, common ware **(3 samples)** and lamps **(8 samples)** of the **Hellenistic-Roman** period from Siracusa [30]; fine unpainted and black glazed pottery from the archaic to the **Hellenistic** period [28] and transport amphorae of VI -V century B.C., from Gela [34]; transport amphorae of VI-V century B.C. from Agrigento [29].

4. Methods

4.1 Characterization of clays and ceramics

Clays were characterized by textural and compositional point of view with the aim to provide a complete characterization of sediments and complement chemical data for the construction of the ANN network. Particle size analyses were carried out to determine particle size distribution; the fraction greater than 32 μm was separated by wet sieving, while **< 32 μm fraction was** obtained by sedimentation.

Mineralogical composition of clay sediments **was** obtained by X-ray diffraction (XRD), using a SIEMENS D5000, with Cu-Kα radiation and Ni-filter. Whole-rock randomly oriented powders were scanned from 5° to 65° 2θ, with a 0.02° 2θ step size and a count time of 2 s per step. The tube current and the voltage were 30 mA and 40 kV, respectively. Oriented slides (<2 μm grain-size fraction) were scanned from 2° to 45° 2θ with a 0.02° 2θ step size and a 4 sec counting time, at 30 mA and 40 kV. The presence of swelling clay minerals was determined by treating samples with ethylene glycol at 60 °C for 12 h. MIF (Mineral Intensity Factor) method was employed to estimate the composition of whole-rock and fine fraction (Ø<2 μm) from XRD patterns [38,39].

Chemical analyses of major and trace elements were performed on clays and ceramics by X-ray fluorescence (XRF) spectrometry (PHILIPS PW 2404/00) on powder-pressed pellets. **In spite of the availability of compositional data from literature, ceramics were reanalyzed to minimize measurement errors and improve the affordability of the method. T**otal loss on ignition (L.O.I.) was gravimetrically estimated after overnight heating at 950 °C. Quantitative analysis was carried out using a calibration line based on 45 international rocks standards. The lower detection limits (LDL) were: SiO_2=1 wt.%, TiO_2=0.01 wt.%, Al_2O_3=0.1 wt.%, Fe_2O_3=0.05 wt.%, MnO=0.01 wt.%, MgO=0.02 wt.%, CaO=0.05 wt.%, Na_2O=0.01 wt.%,K_2O=0.05 wt.%, P_2O_5=0.01 wt.%, Cr=5 ppm, Ni=5 ppm, Zn=15 ppm, Rb=5 ppm, Sr=10 ppm, Y=3 pm, Zr=20 ppm, La=5 ppm, Ce=10 ppm. The precision was monitored by routinely running a well-investigated house standard (obsidian). The average relative standard deviations (RDS%) were less than 5%. Finally, accuracy was evaluated using an international standard that is compositional similar to the samples analysed. Accuracy was good for major elements (<3%) except MnO, and for trace elements (≤5%).

4.2 Creation of clay mixing and feed forward ANN

Chemical compositional data obtained **by XRF** on clays were used to create mathematical clay mixings, keeping in consideration all the possible triplets of samples and varying the mass fraction of 20% following the equation

$$C_M = x \cdot C_a + y \cdot C_b + z \cdot C_c \qquad (6)$$

in which: C_M = composition of calculated clay mixing; C_a, C_b and C_c = compositions of three randomly selected clay samples (*a*,*b* and *c*); *x*, *y* and *z* = mass fractions each varying in turns 0.2, 0.4, 0.6, 0.8 and calculated so that $x + y + z = 1$.

Among of all the obtained **mixings**, 5000 C_M samples for each site (30000 samples considering the six sites) were randomly selected. **T**he frequency distribution in the compositional space of calculated mixed samples reflects**, thus,** the original distribution of the sampled clayey sediments**; in this way,** the mixed samples **are** more numerous near clusters of end members and conversely sparse where there are not clusters of end members. **The 30000 clay sediment mixings were therefore used to train the ANN; the input analysis was given by a standardization function $[X - \overline{X}/\sigma]$ (where $\overline{X}$ is the mean value and σ is the standard deviation), while the output layer was due to the six investigated sites (Agrigento, Catania, Gela, Lentini, Milazzo and Siracusa).** A Multilayer Perceptron Model (MLP) was applied to construct a feed forward neural network **by SPSS version 23.0.0.0 software [40]**.

5. Results and Discussion

5.1 Clays characterization

Chemical composition of studied sediments (see Table S1) is quite variable, even within the same outcropping area. On average, Milazzo samples exhibit the higher **amount** in Rb than the other Plio-Pleistocene sediments, while clays from Catania and Lentini are characterized by the highest Cr and Fe_2O_3 values **(Figure 4)**. In spite of these trends, due to the compositional variability within the same locality, wide overlapping areas are evident (**see** Figure 4).

The textural and mineralogical characterization of clays allows better defining the whole features of studied sediments and complementing chemical data, supporting evidences about similarities among samples from different areas (Figure S1). As far as texture [41], it mainly ranges from silty clay to clayey silt, along with few samples classified as clay + silt + sand, regardless geographic location and/or stratigraphic position of samples. Bulk rocks mineralogical composition is dominated by clay minerals (mean = 43.1; Dev. St. = 12.0), quartz (mean = 23.3; Dev. St. = 7.6) and calcite (mean = 25.2; Dev. St. = 10.4), with subordinate feldspars (mean = 6.9; Dev. St. = 4.6). **A** higher level of clay minerals and feldspars **is** shown by Catania and Milazzo samples, respectively, while Siracusa and Gela clays are **on average** rich**er** in calcite. As regard the fine fraction (< 2 mm), in all samples clay**s are mainly due to** smectite (mean = 50.0; Dev. St. = 11.9), **along with** illite (mean = 21.0; Dev. St. = 7.2) kaolinite (mean = 19.9; Dev. St. = 6.3), and chlorite (mean = 5.3; Dev. St. = 2.1).

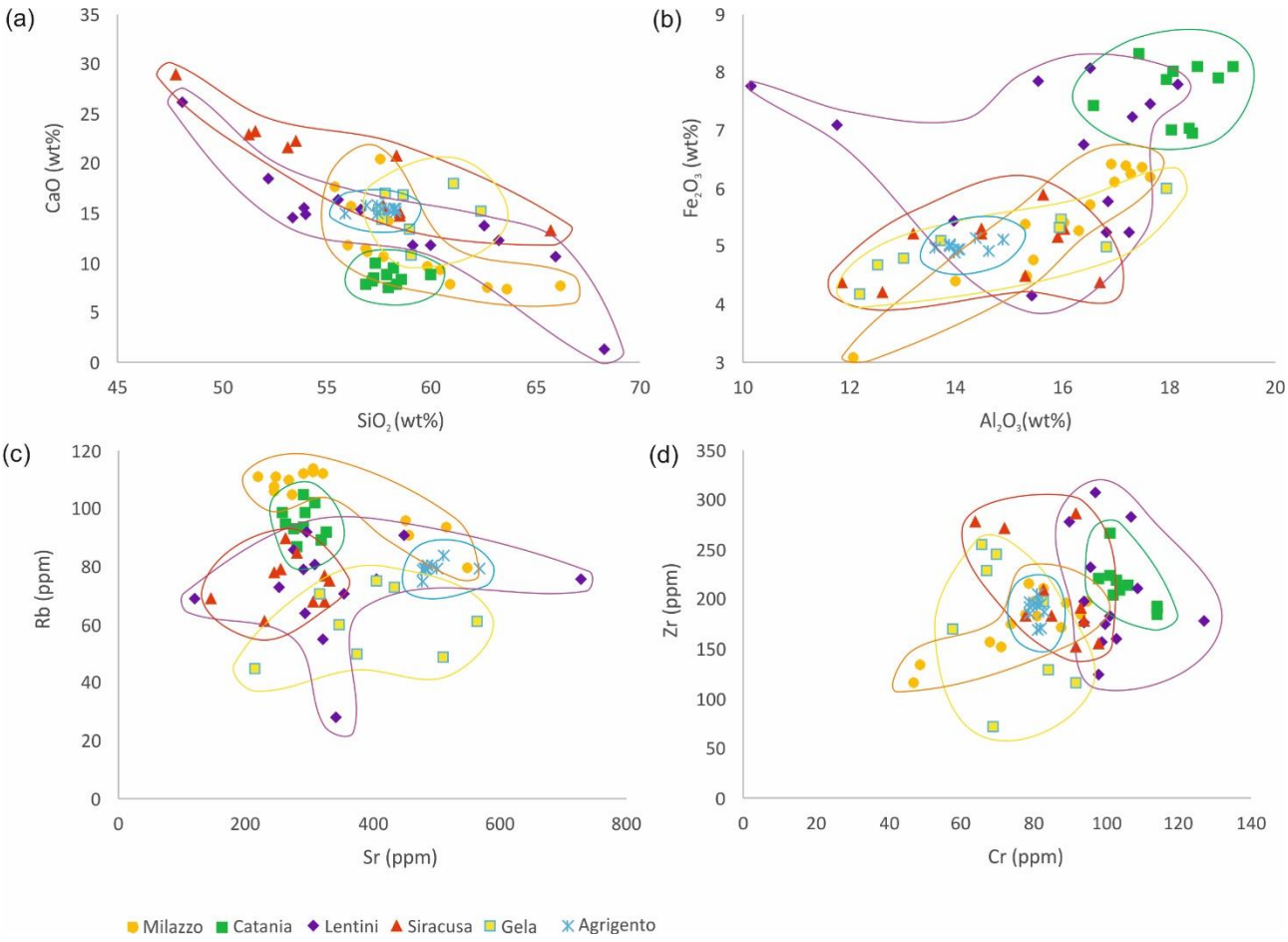

Figure 4. Examples of binary diagrams of major **elements (a)** SiO_2 vs CaO and **(b)** Fe_2O_3 vs Al_2O_3**. Binary diagrams of** trace **elements** (**c)** Rb vs Sr and **(d)** Zr vs Cr **relevant in showing compositional overlapping fields** for clay sediments.

5.2 Classical statistical analysis

In order to propose a cross-validation, classical **statistical** methods were applied to the mathematically created clay mixings.

Firstly, principal component analysis (PCA) was performed considering trace elements**, expressing the major variance**. The rotated varimax principal components diagrams are reported in Figure 5. **As a result,** Lentini and Catania clay sediment **mixe**s accounts the higher PC1 score, while Milazzo **mixes** are controlled by PC3. Beside these discriminating criteria, the other Plio-Pleistocenic clay **mixe**s show largely overlapped plot fields.

An overall, the calculated first three principal components (PC) describe the 74.7% of the total variance.

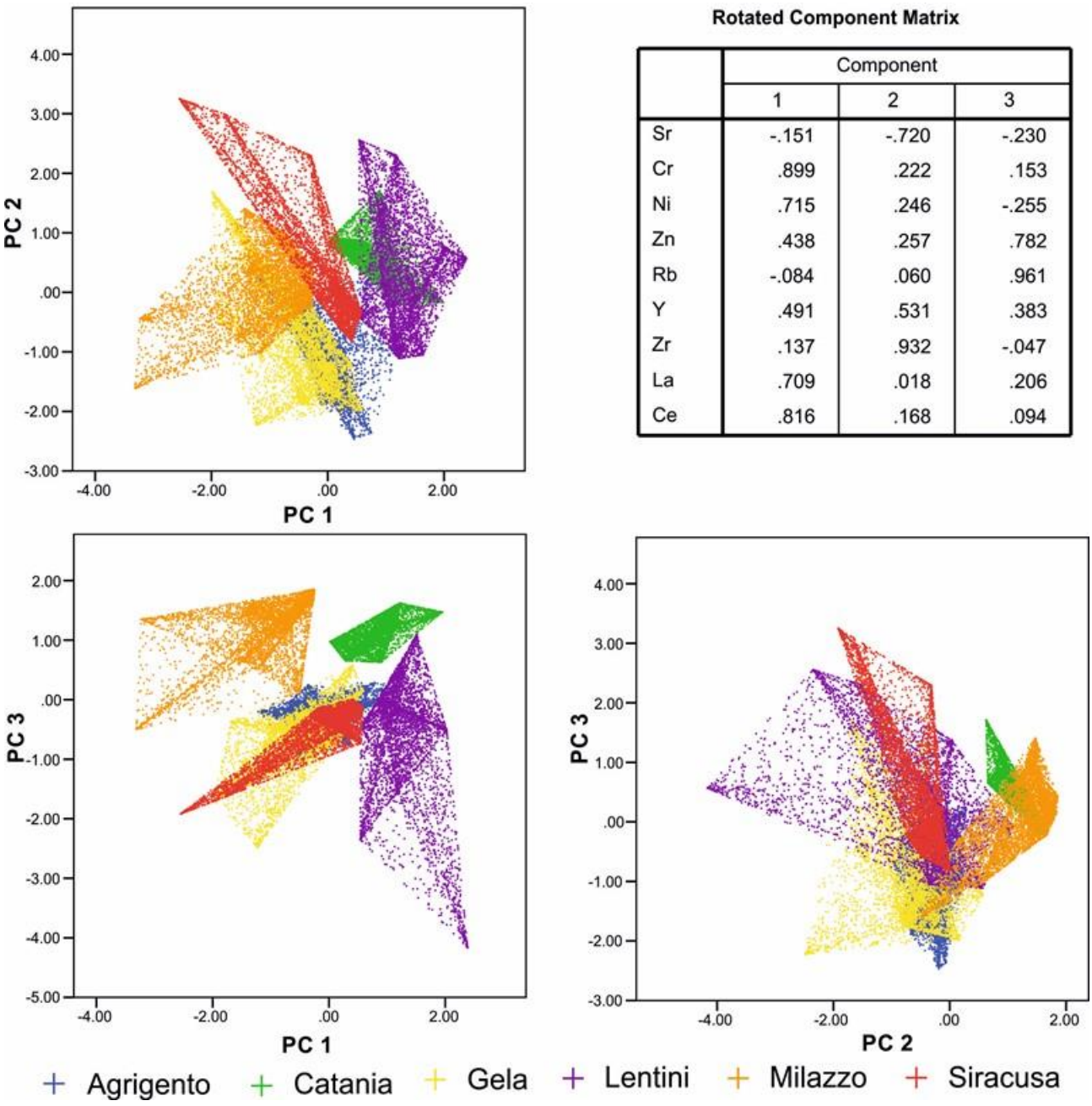

Rotated Component Matrix

	Component		
	1	2	3
Sr	-.151	-.720	-.230
Cr	.899	.222	.153
Ni	.715	.246	-.255
Zn	.438	.257	.782
Rb	-.084	.060	.961
Y	.491	.531	.383
Zr	.137	.932	-.047
La	.709	.018	.206
Ce	.816	.168	.094

Figure 5. Plots of the first three principal component (PC) obtained by the multivariate statistical analysis of **the 30000 mathematically created clay mixes (5000 for each site).** In table, the weights of PC accounting trace elements are reported.

Secondly, linear **discriminant analysis** was applied to the clay mixings, considering also in this case trace element **content**. The **obtained** Discriminant Functions (DF) **are reported in Table 1.**

Discriminant function	Chemical element weights expressing the new variables
1DF	**Sr = -0.070, Cr = 0.569, Ni = 0-.302, Zn = 0-.034, Rb = -1.158, Y = -0.294, Zr = 0.336, La = 0.473, Ce = 0.594**
2DF	**Sr = -0.329, Cr = 0.575, Ni = -0.198, Zn = 0.751, Rb = 0.030, Y = -0.247, Zr = 0.366, La = -0.277, Ce = -0.031**

3DF	**Sr = 0.782, Cr = 0.561, Ni = -0.461, Zn = 0.622, Rb = -0.440, Y = 0.264, Zr = -0.202, La = -0.351, Ce = -0.204**
4DF	**Sr = -0.128, Cr = -0.578, Ni = 0.989, Zn = -0.313, Rb = 0.204, Y = 0.903, Zr = -0.763, La = -0.234, Ce = 0.461**
5DF	**Sr = 0.018, Cr = 0.589, Ni = -0.372, Zn = -0.838, Rb = 0.529, Y = 0.679, Zr = -0.077, La = 0.203, Ce = -0.176**

Table 1. Discriminant functions obtained by LDA analysis.

LDA seems to improve provisional attribution, with **an average** 91.5% of **correct classification,** as reported in Table 2.

	Predicted site					
	Agrigento	Catania	Gela	Lentini	Milazzo	Siracusa
Agrigento	**4698 (94.0%)**	0 (0.0%)	224 (4.5%)	76 (1.5%)	0 (0.0%)	0 (0.0%)
Catania	0 (0.0%)	**5000 (100.0%)**	0 (0.0%)	0 (0.0%)	0 (0.0%)	0 (0.0%)
Gela	1499 (30.0%)	121 (2.4%)	**2896 (57.9%)**	0 (0.0%)	0 (0.0%)	484 (9.7%)
Lentini	77 (1.5%)	0 (0.0%)	0 (0.0%)	**4843 (96.9%)**	0 (0.0%)	80 (1.6%)
Milazzo	0 (0.0%)	0 (0.0%)	0 (0.0%)	0 (0.0%)	**5000 (100.0%)**	0 (0.0%)
Siracusa	0 (0.0%)	0 (0.0%)	0 (0.0%)	0 (0.0%)	0 (0.0%)	**5000 (100.0%)**

Table 2. LDA based **provenance classification** for clay sediments mixes

5.3 ANN network

After numerous trials, the best architecture **for the ANN** was pinpointed in a not excessively restrictive network, consisting in one hidden layer of 5 units (neurons) **able to clearly** separate **the mathematically constructed mixes during the learning procedure** [42]. The transfer function used in the back propagation (BP) optimization algorithm to produce the output was a hyperbolic tangent ($f(x) = \tanh(x) = 2/1 + e^{-2x} - 1$) [43] while for output layer, softmax ($f(x) = e_i^x / \sum_{m=1}^{M} e_m^x$) and cross-entropy were used as transfer and error functions**, respectively**.

Once the best MLP was established, a multiple averaging method was applied to refine the network and assure predictions based on robust data; it consists in repeating the analysis run several times, by changing each time the input order of variables and evaluating the averaging probability obtained. After eleven runs (Figure 6.a), the network reaches the 95 % of correct prediction in training and the 75.5% in testing (see Table 3), with a plateau of the values after the first three runs (see Figure 6.b). Noteworthy is that Rb, and secondary Cr and Sr, seem to have the greater importance in input weights, as shown in Figure 6.c.

	Training		***Testing***	
Number of run	***Cross Entropy Error***	***Percent correct Predictions***	***Cross Entropy Error***	***Percent correct Predictions***
1	14997	84.9%	97	70.3%
2	10610	81.7%	106	72.9%
3	4180	95.9%	136	67.0%
4	11378	90.7%	107	66.1%
5	8918	86.7%	135	59.3%

6	9665	89.7%	132	61.8%
7	11910	85.1%	139	54.3%
8	10010	92.3%	136	65.2%
9	2904	96.4%	151	67.0%
10	6556	92.1%	118	73.7%
11	5051	95.0%	141	75.5%

Table 3. Prediction and relative errors for each training and testing runs performed during the optimization of the ANN.

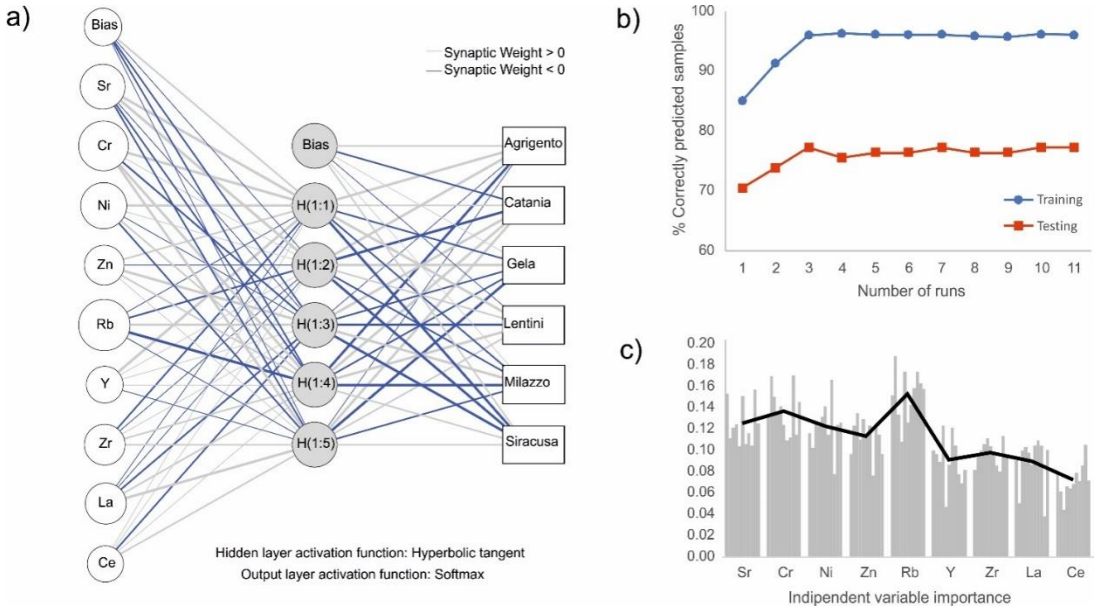

Figure 6. (a) Example of ANN architecture after eleven training run. (b) Affordability of predictions in function of number of training and testing runs. (c) Importance of independent variable as inputs of the constructed ANN.

The extremely flexibility of such computational model allows the application of correction factors to improve the role of the activation function in creating correct correlations. The Bayesian probability factor allows to refine the correlation activated by neurons by assigning a M class {C_i: i = 1.. . . . M} to an input vector X with elements {x_i: i = 1.. . . . D}. Minimum-error Bayesian classifiers perform this task by calculating the Bayesian probability $p(C_i|X)$ for each class, and assigning the input to the class with the highest Bayesian probability, expressed as:

$$p(C_i|X) = p(X|C_i)p(C_i)/p(X) \qquad (7)$$

where $p(X|C_i)$ is the conditional probability of producing the input if the class is C_i, $p(C_i)$ is the a priori probability of class C_i, and $p(X)$ is the unconditional probability of the input.

The possibility to use a correction factor is particularly relevant in archaeological studies, improving the output of the testing procedure by considering archaeological, historical and geographic variables. In this prospective, a Bayesian probability correction factor Y_{ij} was applied to the constructed ANN to provide a refinement of the provisional attribution based on the clay mixes:

$$p(C_i|X)_{cor} = p(C_i|X)Y_{ij} \qquad (8)$$

With values ranging from 0 to 1, it accounts the probability that a sample *X* found in the site *i* is produced in the site *j*.

In order to validate the constructed artificial neural network and evaluate the merits of the method in comparison with classical statistical analysis, LDA, PCA and **the constructed** ANN **learned by clay sediment mixes** were **applied** on **archaeological ceramics compositional data** (see Table **S2**).

The principal component analysis carried out on the 118 selected potteries showed that the first three PC explain 79.5% of the total variance, with evident overlapping of the different provenance fields (Figure 7, Table 4).

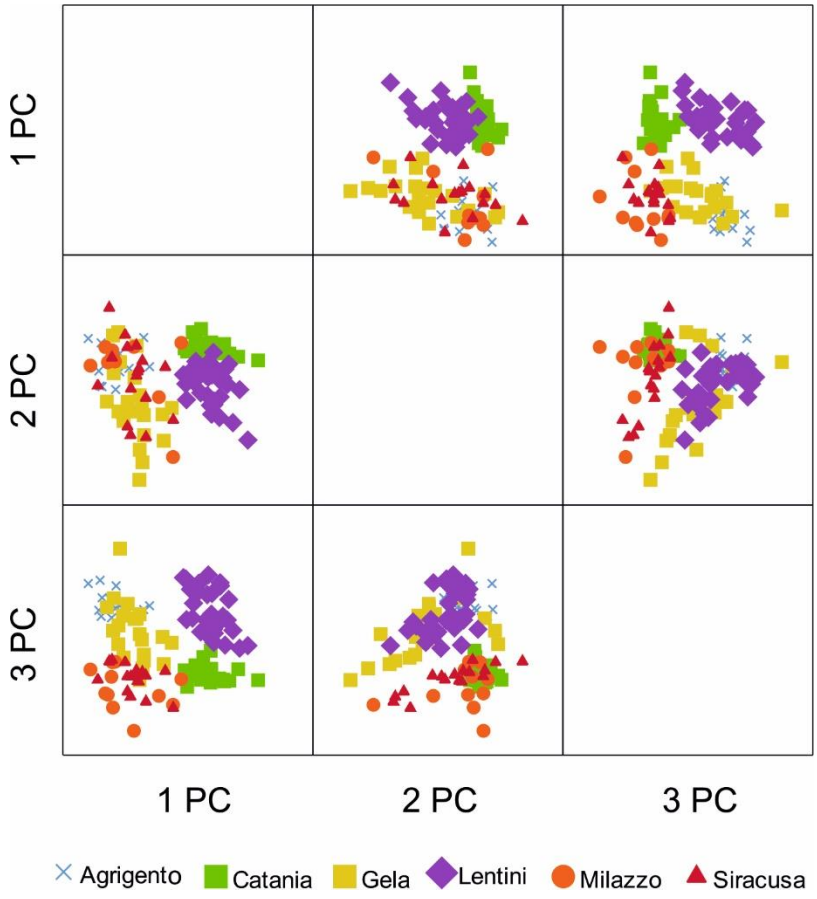

Figure 7. Plots of the first three principal component (PC) obtained by the multivariate statistical analysis of studied potteries.

	Components		
	PC 1	**PC 2**	**PC 3**
Sr	**0.05**	**0.13**	**0.95**
Cr	**0.90**	**0.22**	**0.14**
Ni	**0.88**	**-0.19**	**0.26**
Zn	**0.90**	**0.13**	**-0.03**
Rb	**0.52**	**0.58**	**-0.14**
Y	**0.28**	**0.87**	**0.18**
Zr	**-0.02**	**0.86**	**0.08**

La	**0.71**	**0.41**	**-0.03**
Ce	**0.75**	**0.34**	**-0.14**

Table 4. Rotated component matrix. Weights of PC accounting trace elements are reported.

As **far as** LDA analysis, DFs were calculated for pottery samples in relation to clay sediments compositional data**; the data processing allows to observe** only a 50% of correct provenance attribution (Table 5).

On the contrary, the **application of ANN** computational model accounts overall the 78% of **correct provenance classification**. In particular, the most accurate provenance attribution is verified for Catania (100%), Lentini (93.8%) and Milazzo (81.8%), while up to 50-60% correct classification is verified for Siracusa, Gela and Agrigento (Table 6), with a general improvement of provisional attribution respect to classical **statistical methods**.

	Predicted site					
	Agrigento	Catania	Gela	Lentini	Milazzo	Siracusa
Agrigento	**4 (26.7%)**	0 (0.0%)	7 (46.7%)	3 (20.0%)	0 (0.0%)	1 (6.7%)
Catania	0 (0.0%)	**21 (100.0%)**	0 (0.0%)	0 (0.0%)	0 (0.0%)	0 (0.0%)
Gela	2 (9.1%)	1 (4.5%)	**7 (31.8%)**	5(22.7%)	0 (0.0%)	7 (31.8%)
Lentini	2 (6.3%)	24 (75.0%)	0 (0.0%)	**5 (15.6%)**	1 (3.1%)	0 (0.0%)
Milazzo	0 (0.0%)	1 (9.1%)	0 (0.0%)	0 (0.0%)	**8 (72.7%)**	2 (18.2%)
Siracusa	0 (0.0%)	0 (0.0%)	0 (0.0%)	3 (17.6%)	0 (0.0%)	**14 (82.4%)**

Table 5. LDA based **provenance classification** for ceramic samples

	Predicted site					
	Agrigento	Catania	Gela	Lentini	Milazzo	Siracusa
Agrigento	**8 (53.3%)**	0 (0.0%)	4 (26.7%)	3 (20.0%)	0 (0.0%)	0 (0.0%)
Catania	0 (0.0%)	**21 (100.0%)**	0 (0.0%)	0 (0.0%)	0 (0.0%)	0 (0.0%)
Gela	3 (13.6%)	0 (0.0%)	**14 (63.6%)**	5 (22.7%)	0 (0.0%)	0 (0.0%)
Lentini	0 (0.0%)	2 (6.3%)	0 (0.0%)	**30 (93.8%)**	0 (0.0%)	0 (0.0%)
Milazzo	0 (0.0%)	1 (9.1%)	0 (0.0%)	0 (0.0%)	**9 (81.8%)**	1 (9.1%)
Siracusa	1 (5.9%)	0 (0.0%)	0 (0.0%)	6 (35.3%)	0 (0.0%)	**10 (58.8%)**
%tot	**78.0%**					

Table 6. **ANN based provenance classification for ceramic samples**

Finally, an improvement of the provisional attribution based on ANN computational model was obtained by the application of correction factors Y_{ij} (Table 7), weighted on the basis of historical and archaeological evidences informing us about political and social relationship among the selected Greek colonies, geographic location, connections, trades route, hostilities vs. and alliances. Taking in account the corrected Bayesian probability in the two different selected scenario (the second scenario more restrictive than the first one), an increasing of the corrected attribution was obtained, from 78% to 81.4% and 88.1%, respectively (see Tables 8 a-b).

(a)	Predicted site					
	Agrigento	Catania	Gela	Lentini	Milazzo	Siracusa
Agrigento	1	0.6	0.8	0.6	0.4	0.4
Catania	0.6	1	0.6	0.8	0.6	0.6
Gela	0.8	0.6	1	0.6	0.4	0.4
Lentini	0.6	0.8	0.6	1	0.6	0.6
Milazzo	0.4	0.4	0.4	0.6	1	0.4
Siracusa	0.4	0.6	0.4	0.4	0.4	1
(b)	Predicted site					
	Agrigento	Catania	Gela	Lentini	Milazzo	Siracusa
Agrigento	1	0.3	0.4	0.3	0.2	0.2
Catania	0.3	1	0.3	0.4	0.3	0.3
Gela	0.4	0.3	1	0.3	0.2	0.2
Lentini	0.3	0.4	0.3	1	0.3	0.3
Milazzo	0.2	0.2	0.2	0.3	1	0.2
Siracusa	0.2	0.3	0.2	0.2	0.2	1

Table 7. Bayesian probability correction factors Y_{ij} for (a) less and (b) more restrictive cases

(a)	Predicted site					
	Agrigento	Catania	Gela	Lentini	Milazzo	Siracusa
Agrigento	**8 (53.3%)**	0 (0.0%)	4 (26.7%)	3 (20.0%)	0 (0.0%)	0 (0.0%)
Catania	0 (0.0%)	**21 (100.0%)**	0 (0.0%)	0 (0.0%)	0 (0.0%)	0 (0.0%)
Gela	3 (13.6%)	0 (0.0%)	**15 (68.2%)**	4 (18.2)	0 (0.0%)	0 (0.0%)
Lentini	2 (6.3%)	0 (0.0%)	0 (0.0%)	**30 (93.8%)**	0 (0.0%)	0 (0.0%)
Milazzo	0 (0.0%)	1 (9.1%)	0 (0.0%)	0 (0.0%)	**10 (90.9%)**	0 (0.0%)
Siracusa	0 (0.0%)	1 (5.9%)	0 (0.0%)	4 (23.5%)	0 (0.0%)	**12 (70.6%)**
%tot	**81.4%**					
(b)	Predicted site					
	Agrigento	Catania	Gela	Lentini	Milazzo	Siracusa
Agrigento	**12 (80.0%)**	0 (0.0%)	1 (6.7%)	2 (13.3%)	0 (0.0%)	0 (0.0)
Catania	0 (0.0%)	**21 (100.0)**	0 (0.0%)	0 (0.0%)	0 (0.0%)	0 (0.0%)
Gela	2 (9.1%)	0 (0.0%)	**16 (72.7%)**	4 (18.2%)	0 (0.0%)	0 (0.0%)
Lentini	0 (0.0%)	1 (3.1%)	0 (0.0%)	**31 (96.9%)**	0 (0.0%)	0 (0.0%)
Milazzo	0 (0.0%)	1 (9.1%)	0 (0.0%)	0 (0.0%)	**10 (90.9%)**	0 (0.0%)
Siracusa	0 (0.0%)	1 (5.9%)	0 (0.0%)	2 (11.8%)	0 (0.0%)	**14 (82.3%)**
%tot	**88.1%**					

Table 8. **A**NN based membership prediction, applying (a) less and (b) more restrictive Bayesian probability **factor**

6. Conclusion

In this work, **mathematically created clay mixes based on a** clay sediment database **were used to** learn an artificial neural network for provisional provenance attribution of archaeological **ceramics**.

As far as the testing process assessed on clays mixes, the obtained results favor the ANN method, suggesting that the computational model allows overpassing the uncertainties of PCA and LDA, especially in the case of wide overlapping compositional **ranges**. Actually, the application of the **learned** ANN **on 30000 clay mixes** gives backs **the** 95% and 75.5% of correct attribution in training and testing procedures, respectively, in view of 74.7% obtained by PCA method; average comparable results are obtained by LDA method, accounting the 91.5% of correct attribution.

The merits of ANN are **particularly** evident when the network is tested with archaeological ceramics; in fact, **in the case of potteries,** the **computation** gives back the 78% of correct **provenance attribution**, improving **predictions** of 28% respect to LDA (accounting the 50% of correct provisional attribution) as well as the discrimination provided by PCA analysis. Moreover, the introduction of **the** Bayesian probability **factor, which takes** in account historical and archaeological **evidences,** allows to largely improve provenance attributions, reinforcing the importance of critically evaluate analytical data.

Thus, it is possible to conclude that if a neural network is properly **learned** and a representative database of reference material is available, ANN is a powerful supervised recognition technique in archaeometric studies. The outcome of the research enlarges therefore the prospective of ANN application as successful method in provenance studies of archaeological ceramics, especially in discriminating production sites characterized by similar cultural and geological characteristics, which are therefore almost indistinguishable both in the morphological-typological aspects and in the macroscopic/microscopic ceramic paste features.

References

[1] M.S. Tite, Ceramic production, provenance and use - A review, Archaeometry. 50 (2008) 216–231. doi:10.1111/j.1475-4754.2008.00391.x.

[2] A.M. Pollard, C. Heron, Archaeological chemistry, Royal Society of Chemistry, 1996.

[3] T.D. Price, J.H. Burton, Archaeological Chemistry, in: An Introd. to Archaeol. Chem., Springer New York, New York, NY, 2011: pp. 1–24. doi:10.1007/978-1-4419-6376-5_1.

[4] D. Miriello, G.M. Crisci, Mixing and provenance of raw materials in the bricks from the Svevian castle of Rocca Imperiale (North Calabria, Italy), Eur. J. Mineral. 19 (2007) 137–144. doi:10.1127/0935-1221/2007/0019-0137.

[5] D. Miriello, A. Bloise, R. De Luca, C. Apollaro, G.M. Crisci, S. Medaglia, A. Taliano Grasso, First compositional evidences on the local production of Dressel 2–4 amphorae in Calabria (Southern Italy): characterization and mixing simulations, Appl. Phys. A. 119 (2015) 1595–1608. doi:10.1007/s00339-015-9143-y.

[6] R.B. Heimann, M. Maggetti, Ancient and historical ceramics: materials, technology, art, and culinary traditions, Schweizerbart Science Publishers, Stuttgart, Germany, 2014.

[7] V. Panchuk, I. Yaroshenko, A. Legin, V. Semenov, D. Kirsanov, Application of chemometric methods to XRF-data – A tutorial review, Anal. Chim. Acta. 1040 (2018) 19–32. doi:10.1016/j.aca.2018.05.023.

[8] F. Bellanti, M. Tomassetti, G. Visco, L. Campanella, A chemometric approach to the historical and geographical characterisation of different terracotta finds, Microchem. J. 88 (2008) 113–120. doi:10.1016/j.microc.2007.11.019.

[9] J.A. Carrero, N. Goienaga, S. Fdez-Ortiz de Vallejuelo, G. Arana, J.M. Madariaga, Classification of archaeological pieces into their respective stratum by a chemometric model based on the soil concentration of 25 selected elements, Spectrochim. Acta - Part B At. Spectrosc. 65 (2010) 279–286. doi:10.1016/j.sab.2010.01.009.

[10] R.G. Giménez, R.V. De La Villa, M.D.P. Domínguez, M.I. Rucandio, Application of chemical, physical and chemometric analytical techniques to the study of ancient ceramic oil lamps, Talanta. 68 (2006) 1236–1246. doi:10.1016/j.talanta.2005.07.033.

[11] G. Barone, A. Lo Giudice, P. Mazzoleni, A. Pezzino, D. Barilaro, V. Crupi, M. Triscari, Chemical characterization and statistical multivariate analysis of ancient pottery from Messina, Catania, Lentini and Siracusa (Sicily), Archaeometry. 47 (2005) 745–762. doi:10.1111/j.1475-4754.2005.00230.x.

[12] D. Seetha, G. Velraj, Characterization and chemometric analysis of ancient pot shards trenched from Arpakkam, Tamil Nadu, India, J. Appl. Res. Technol. 14 (2016) 345–353. doi:10.1016/j.jart.2016.08.002.

[13] P. Fermo, E. Delnevo, M. Lasagni, S. Polla, M. de Vos, Application of chemical and chemometric analytical techniques to the study of ancient ceramics from Dougga (Tunisia), Microchem. J. 88 (2008) 150–159. doi:10.1016/j.microc.2007.11.012.

[14] P. Fermo, F. Cariati, D. Ballabio, V. Consonni, G.B. Gianni, Classification of ancient Etruscan ceramics using statistical multivariate analysis of data, Appl. Phys. A Mater. Sci. Process. 79 (2004) 299–307. doi:10.1007/s00339-004-2520-6.

[15] R. Aruga, P. Mirti, A. Casoli, Application of multivariate chemometric techniques to the study of Roman pottery (terra sigillata), Anal. Chim. Acta. 276 (1993) 197–204. doi:10.1016/0003-2670(93)85056-P.

[16] J.A. Remolà, J. Lozano, I. Ruisánchez, M.S. Larrechi, F.X. Rius, J. Zupan, New chemometric tools to study the origin of amphorae produced in the Roman Empire, TrAC - Trends Anal. Chem. 15 (1996) 137–151. doi:10.1016/0165-9936(95)00091-7.

[17] G.E. De Benedetto, B. Fabbri, S. Gualtieri, L. Sabbatini, P.G. Zambonin, FTIR-chemometric tools as aids for data reduction and classification of pre-Roman ceramics, J. Cult. Herit. 6 (2005) 205–211. doi:10.1016/j.culher.2005.06.004.

[18] L. Rampazzi, A. Pozzi, A. Sansonetti, L. Toniolo, B. Giussani, A chemometric approach to the characterisation of historical mortars, Cem. Concr. Res. 36 (2006) 1108–1114. doi:10.1016/j.cemconres.2006.02.002.

[19] A. De Bonis, S. Febbraro, C. Germinario, D. Giampaola, C. Grifa, V. Guarino, A. Langella, V. Morra, Distinctive Volcanic Material for the Production of Campana A Ware: The Workshop Area of Neapolis at the Duomo Metro Station in Naples, Italy, Geoarchaeology. 31 (2016) 437–466. doi:10.1002/gea.21571.

[20] A. Aprile, G. Castellano, G. Eramo, Combining image analysis and modular neural networks for classification of mineral inclusions and pores in archaeological potsherds, J. Archaeol. Sci. 50 (2014) 262–272. doi:10.1016/J.JAS.2014.07.017.

[21] A. Ramil, A.J. López, A. Yáñez, Application of artificial neural networks for the rapid classification of archaeological ceramics by means of laser induced breakdown spectroscopy (LIBS), Appl. Phys. A Mater. Sci. Process. 92 (2008) 197–202. doi:10.1007/s00339-008-4481-7.

[22] S. Pagnotta, S. Legnaioli, B. Campanella, E. Grifoni, M. Lezzerini, G. Lorenzetti, V. Palleschi, F. Poggialini, S. Raneri, Micro-chemical evaluation of ancient potsherds by μ-LIBS scanning on thin section negatives, Mediterr. Archaeol. Archaeom. 18 (2018) 171–178. doi:10.5281/zenodo.1285906.

[23] J. Qi, T. Zhang, H. Tang, H. Li, Rapid classification of archaeological ceramics via laser-induced breakdown spectroscopy coupled with random forest, Spectrochim. Acta Part B At. Spectrosc. 149 (2018) 288–293. doi:10.1016/J.SAB.2018.09.006.

[24] W.S. McCulloch, W. Pitts, A logical calculus of the ideas immanent in nervous activity, Bull. Math. Biophys. 5 (1943) 115–133. doi:10.1007/BF02478259.

[25] S. Haykin, Adaptive Filters, Signal Process. Mag. 6 (1999) 1–6.

[26] D.E. Rumelhart, J.L. McClelland, S.D.P.R.G. University of California, Parallel distributed processing: explorations in the microstructure of cognition, MIT Press, 1986.

[27] M.J. Baxter, Mathematics, statistics and archaeometry: The past 50 years or so, Archaeometry. 50 (2008) 968–982. doi:10.1111/j.1475-4754.2008.00427.x.

[28] E. Aquilia, G. Barone, P. Mazzoleni, C. Ingoglia, Petrographic and chemical characterisation of fine ware from three Archaic and Hellenistic kilns in Gela, Sicily, J. Cult. Herit. 13 (2012) 442–447. doi:10.1016/j.culher.2012.02.005.

[29] G. Barone, C. Branca, V. Crupi, S. Ioppolo, D. Majolino, G. Puglisi, G. Spagnolo, G. Tigano, Archaeometric analyses on ceramics from Sicilian Greek colonies: A contribution to the knowledge of Messina, Gela and Agrigento production, Period. Di Mineral. 73 (2004) 43–56.

[30] G. Barone, P. Mazzoleni, A. Aquilia, G. Barbera, The hellenistic and Roman syracuse (sicily) fine pottery production explored by chemical and petrographic analysis, Archaeometry. 56 (2014) 70–87. doi:10.1111/j.1475-4754.2012.00727.x.

[31] G. Barone, V. Crupi, D. Majolino, P. Mazzoleni, J. Teixeira, V. Venuti, Small angle neutron scattering as fingerprinting of ancient potteries from Sicily (Southern Italy), J. Appl. Phys. 106 (2009) 1–26.

[32] G. Barone, P. Mazzoleni, C. Ingoglia, M.G. Vanaria, Archaeometric evidences of the 4th-2nd century BC amphorae productions in north eastern Sicily, J. Archaeol. Sci. 38 (2011) 3060–3071.

[33] G. Barone, P. Mazzoleni, G. Spagnolo, E. Aquilia, The transport amphorae of Gela: A multidisciplinary study on provenance and technological aspects, J. Archaeol. Sci. 39 (2012) 11–22.

[34] G. Barone, Preliminary archaeometric analysis on amphorae, in VI and v centuries B.C., from

excavations at Gela (Sicily), Period. Di Mineral. 71 (2002) 273–287.

[35] G. Barone, C. Belfiore, P. Mazzoleni, A. Pezzino, C. Ingoglia, A. Ollà, G. Spagnolo, G. Tigano, Indagini archeometriche su reperti ceramici da Milazzo, in: G. Tigano (Ed.), Milay II – Scavi E Ric. Nell'area Urbana 1996-2005, Sicania, Messina, 2009: pp. 273–301.

[36] M. Grasso, The Appenninic-Maghrebian orogen in southern Italy and adjacent areas, in: Anat. an Orogen - Appennines Adjac. Mediterr. Basins, Kluwer Academic Publishers, 2001.

[37] F. Lentini, S. Carbone, Geologia della Sicilia, ISPRA, 2014.

[38] Moore, R. Jr, X-ray diffraction and the identification and analysis of clay minerals, (1989).

[39] F.L. Lynch, Mineralogy of Frio formation shale and the stoichiometry of the smectite to illite reaction-the most important reaction in clastic sedimentary diagenesis, Clays Clay Miner. 45 (1997) 618–631. doi:10.1346/CCMN.1997.0450502.

[40] IBM, SPSS Neural Networks 23, 2011.

[41] F.P. Francis P. Shepard, Nomenclature Based on Sand-silt-clay Ratios, SEPM J. Sediment. Res. Vol. 24 (1954) 151–158. doi:10.1306/D4269774-2B26-11D7-8648000102C1865D.

[42] S. Knerr, L. Personnaz, G. Dreyfus, Single-layer learning revisited: a stepwise procedure for building and training a neural network, in: F.F. Soulié, J. Hérault (Eds.), Neurocomputing Algorithms, Archit. Appl., Springer Berlin Heidelberg, Berlin, Heidelberg, 1990: pp. 41–50. doi:10.1007/978-3-642-76153-9_5.

[43] M. Otto, Chemometrics: Statistics and Computer Application in Analytical Chemistry, Wiley, Weinheim, 1999.

Supplementary materials

Figure S1. (a) Sand – Clay – Silt triangular plot (**[41]**). The gray area includes grain size of analysed clay sediments. (b) Bulk and (c) <2 mm grain size fraction mineralogical composition of clay sediments grouped by geographic location **(feld: feldspar; qtz: quartz; c.m.: clay minerals)**.

Table S1. Major and trace elements chemistry of clay sediments used to create clay mixes obtained by XRF analysis. Data are normalized to 100% on LOI-free basis.

Table S2. Chemical composition of selected potteries obtained by XRF analysis. Major and minor elements are expressed in wt% and ppm, respectively. Data are normalized to 100% on LOI-free basis.